Dynamical in situ nuclear-magnetic-resonance tensile apparatus

Hackelöer, H.J.; Kanert, O.; Tamler, H.; De Hosson, J.Th.M.

Published in:
Review of Scientific Instruments

DOI:
10.1063/1.1137370

Publication date:
1983

Dynamical *in situ* nuclear-magnetic-resonance tensile apparatus

H. J. Hackelöer, O. Kanert, and H. Tamler

Institute of Physics, University of Dortmund, 46 Dortmund 50, Federal Republic of Germany

J. Th. M. De Hosson

Department of Applied Physics, Materials Science Centre, University of Groningen, Nijenborgh 18, 9747 AG Groningen, The Netherlands

(Received 29 July 1982; accepted for publication 21 November 1982)

A combination of a servohydraulic tensile machine and NMR pulse spectrometer is described enabling nuclear-spin relaxation rates to be recorded simultaneously with stress-strain data incorporating tension as well as compression of nonmetallic as well as of metallic samples. The data of the mechanical system are as follows: Maximum load: 5000 N; minimum deformation speed: 10 μm s^{-1}, maximum deformation speed: 3×10^5 μm s^{-1}; deformation stroke: digitally controlled between 1 and 8×10^3 μm; bandwidth: dc to 1 kHz; resolution: 2–4 μm; temperature conditions of the sample: from 80 to 570 K. The operation and performance of the system is described by means of experiments observing nuclear-spin relaxation rates which are induced by the movement of dislocations due to the finite deformation rate of the sample.

PACS numbers: 07.58. + g

INTRODUCTION

Every plastic deformation of a solid causes internal microscopic motions such as movements of dislocations or rearrangements of stretched molecules in polymers while the specimen is deforming with a finite rate of deformation.

Using suitable nuclear spins as local probes in the sample the microscopic motions may be observed via additional nuclear-spin relaxation rate induced by such internal motions. Then, by means of standard nuclear-spin relaxation theories, an evaluation of the relaxation data leads to a detailed insight into the dynamics of the microscopic process of the internal motion. In particular, correlation times of the motional process and mean jump distances of atoms, molecules, and lattice defects, respectively, which are involved in the microscopic process of motion, can be obtained by means of such experiments.

In the past we have applied the method for *in situ* investigations of dislocation motion in nonmetallic[1,2] as well as in metallic samples.[3,4] While deforming a sample with a strain rate $\dot{\epsilon}$ the spin lattice relaxation rate in a weak rotating field H_1 ("locking field"[5]), $1/T_{1\rho}$ of the resonant nuclei in the sample is enhanced due to the motion of dislocations. Generally the resulting total relaxation rate may be decomposed into a background relaxation rate, $(1/T_{1\rho})_0$ and the contribution $(1/T_{1\rho})_{\dot{\epsilon}}$ which is governed by the mechanism of the deformation process

$$\frac{1}{T_{1\rho}} = \left(\frac{1}{T_{1\rho}}\right)_0 + \left(\frac{1}{T_{1\rho}}\right)_{\dot{\epsilon}}. \tag{1}$$

In the case of dislocation motion, we have shown, that $(1/T_{1\rho})_{\dot{\epsilon}}$ is caused by time fluctuations of the electric field gradient of mobile dislocations resulting in a nuclear spin relaxation via nuclear quadrupolar interaction for spin with $I > \frac{1}{2}$,[6] but such investigations may easily be carried out to analyze *in situ* the dynamical behavior of other types of internal motions occurring during a plastic deformation. An example of such an experiment is the observation of the dynamics of an alignment process of molecules in a polymer during an external deformation.

It is the aim of this report to present the details of a multiple-purpose tensile testing system operating in combination with a commercial NMR pulse spectrometer which permits *in situ* deformation of samples within the radio-frequency coil of the spectrometer while measuring the NMR signal and nuclear-spin relaxation rates of nuclei in the specimen. It should be noted that most of the elements of the system described here are of commercial type. In addition, the whole device operates for a considerable time without any trouble.

I. DESIGN OF THE SYSTEM

The general setup of the whole tensile testing system is shown in the block diagram of Fig. 1. The device consists of commercial servohydraulic deformation equipment (ZONIC Technical Lab. Inc., Cincinnati, Missouri), a BRUKER NMR pulse spectrometer (SXP4-100), and a data processing system. The tensile machine as well as the NMR spectrometer are controlled by a digital function generator (see also Fig. 2). In the NMR experiment, the sample inside the rf coil is deformed by a driving rod which is the actual output device of the exciter head XCI TE 1105. The major function of the exciter head is to apply a controlled static force and/or a time-varying dynamic force to the rod. This can be done in two different modes of operation. For load control applications, a com-

 0034-6748/83/030341-05$01.30

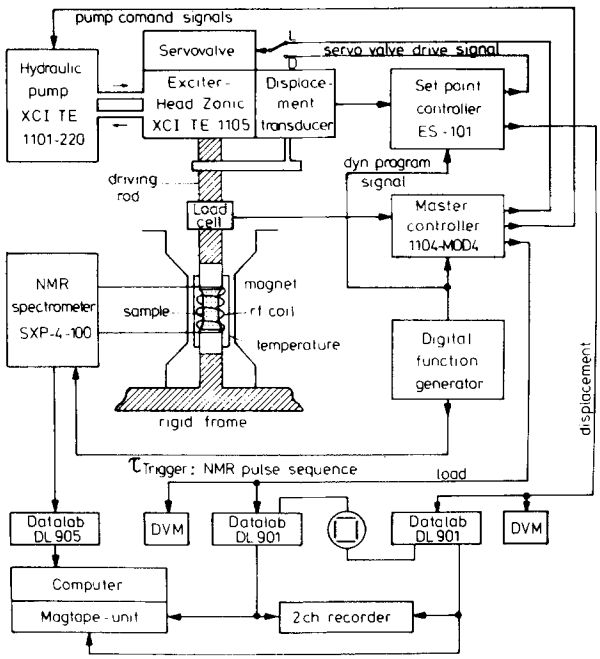

FIG. 1. Block diagram of the digital function generator. The generator controls the tensile machine as well as the pulse spectrometer (see Fig. 2).

bined static and dynamic feedback signal is obtained from the load cell and master controller which serves the servovalve of the exciter head when switch is in position "L" (load). The actual load $P(t)$ is controlled by the dynamical program signal generated by the digital function generator (see also Fig. 2). In position "D" (displacement) of the switch, the displacement $\Delta x(t)$ of the rod is controlled by the dynamical program signal of the digital function generator which serves the set point controller ES-101 in order to generate an error signal which is fed into the servovalve. In that mode, the master controller acts only as a simple load cell amplifier. Furthermore, the master controller adjusts the pressure of the hydraulic power supply 1101-220 via the pump command signals in order to supply the servovalve of the exciter head with a constant pressure of 250 bar. Additional controls for starting and stopping the hydraulic pump are also provided.

During the deformation experiment, the acting load $P(t)$ as well as the resulting displacement $\Delta x(t)$ are measured separately and simultaneously. Both sets of data can be stored in fast transient recorders (DATALAB DL 901), recorded on a two-channel recorder, or transcribed on magnetic tape for further processing of the data by means of an on-line computer.

The data of the mechanical system are as follows: Maximum load: 5000 N; minimum piston speed: 10 μm/s; maximum piston speed: 3×10^5 μm/s; stroke of the piston: digital controlled between 1 and 8000 μm. Resolution (depending slightly on the gain of the electrohydraulic feedback system): 2–4 μm; bandwidth of the system: dc to 1000 Hz.

Figure 2 exhibits further details of the digital function generator which generates the dynamical program signal for both the Master Controller and the Setpoint controller. The heart of the generator consists of a 16-bit up/down BCD counter followed by a 16-bit digital-to-analog converter which generates the dynamical program signal. The velocity preset unit serves the counter with a variable clock frequency which determines the actual slope of the program signal. The clock frequency is derived either from the internal or from an external 10-Hz master frequency. The central control board in connection with the corresponding units shown in Fig. 2 offers the following options: selection of the type of program function (ramp, triangular, sinusoidal) including the option single or periodic; absolute preset of the initial (A) and final position (B) of the piston indicated in μm; start, stop, and reset selection of the function generator; variable delayed trigger signal (τ_{Trigger}) in order to start the NMR experiment at a definite time during the deformation process determined by the delay time of the trigger pulse. As in the case of the mechanical data the different NMR signals were stored in a fast transient recorder (DATALAB DL 905) and then transferred to magnetic tape for further analysis (see also Fig. 1). An example of such a combined

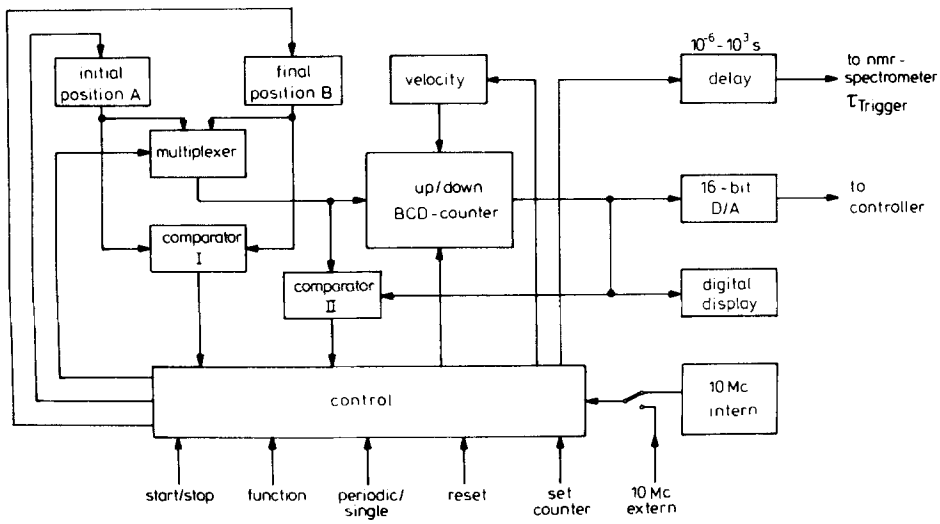

FIG. 2. Block diagram of the experimental setup consisting of servo-hydraulic deformation equipment, an NMR pulse spectrometer including a magnet, and a data processing system.

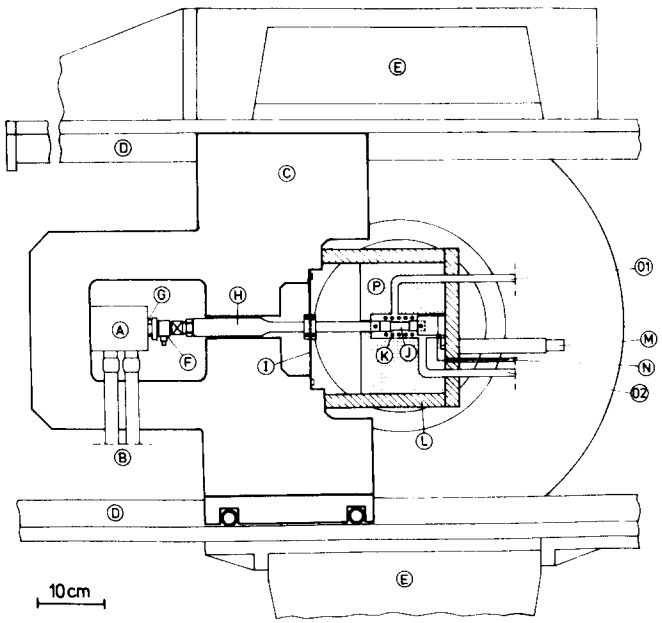

FIG. 3. Sketch of version I of the hydraulic deformation system adaptable to electromagnets. (A) Exciter head including servovalve, (B) connection to hydraulic power supply, (C) movable main frame, (D) upper/lower rail, (E) magnet, (F) load cell, (G) displacement transducer, (H) driving rod, (I) diaphragm (lateral support of the rod), (J) sample, (K) rf sample coil, (L) inner frame, (M) variable tuning capacitor, (N) 50 Ω rf connection, (O) gas flow connection (in: 01; out: 02) for temperature control, (P) Dewar-like heat shield.

deformation-NMR experiment will be given in the next section.

Two different types of frames were designed to contain the temperature controlled NMR probe head consisting of the rf coil and tuning elements as well as the exciter head and the driving piston including the load cell and the displacement transducer. Version I was developed for inserting the frame between the pole pieces of an electromagnet with an air gap of 4 cm, whereas version II could be attached to a wide-bore (8.8 cm) superconducting magnet.

Figure 3 shows a sketch of version I of the frame. The main frame C can be moved on the upper and lower rails D from a preparing position outside the electromagnet into a measuring position where the sample J is situated in the center of the magnet gap. The driving rod H is connected to the piston of the exciter head A via the load cell F and the displacement transducer G. The distance between the rod and the frame is fixed by a diaphragm I with a large stiffness perpendicular to the rod axis and a low stiffness in the displacement direction. The diaphragm prevents the bar from buckling, up to the maximum load of the exciter head. In the deformation experiment the moving rod deforms the sample which is fixed on the inner frame L of the device. In addition, the top of the inner frame L bears the different supply connections, namely rf connection N, input 01 and output connection 02 for the temperature-controlled gas flow, and thermocouple connection (not drawn in Fig. 3).

All parts of the apparatus are manufactured from nonmagnetic materials, mainly from aluminum, and are of sufficiently rigid structure to prevent any mechanical vibration which would perturb the tensile experiment or increase the noise level of the spectrometer.

Coaxially with the specimen J the rf probe coil K is mounted. One side of the coil is connected to the coaxial single-grounded capacitor M which can be tuned by shifting a hollow polyvinylchloride cylinder inside the coaxial capacitor. The other side of the coil can be connected via the 50 Ω output N to further matching elements and to the NMR pulse spectrometer. Further details of optimal tuning of the resonant circuit may be obtained from the book of Fukushima and Roeder about NMR techniques and practical advice in performing NMR experiments.[7]

For accurate temperature control a variable gas-flow temperature accessory including a controller is used. Commonly nitrogen was used as the temperature-regulating gas. Prior to entering the input connection 01, the stream of gas is cooled down or heated up to a preset value between 80 and 570 K with an accuracy of about ±2 K. For that purpose, a temperature sensor downstream from the heat exchanger operates as part of a feedback loop controlling the heater. Depending on the temperature desired, the nitrogen may be generated as boil off from a tank of liquid nitrogen or obtained from a gas cylinder. The actual temperature of the sample is deter-

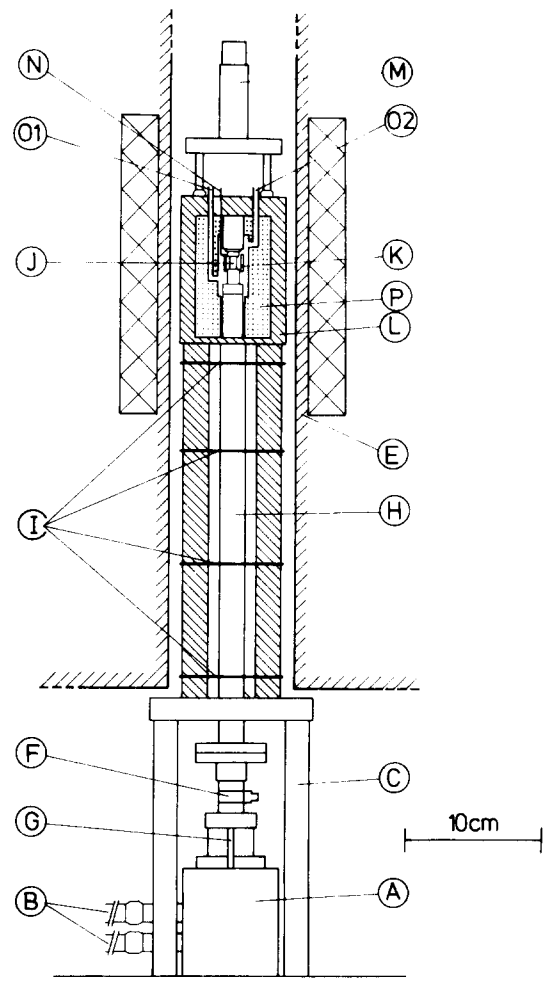

FIG. 4. Sketch of version II of the hydraulic deformation system adaptable to wide-bore (8.8 cm) superconducting magnets. The individual elements are labeled with the same symbols as given in Fig. 3.

mined by a thermocouple placed in contact with the sample. The sample is thermally isolated by the Dewar-like heat shield P manufactured from two pieces of the machinable ceramic material pyrophylite which form two shell-shaped parts of the shield. Additionally, for measurements above 300 K, the outer part of the sample chamber has to be cooled by coolant water (not drawn in Fig. 3).

In Fig. 4, a sketch of version II of the frame adaptable to a superconducting magnet is depicted. If we ignore the fact that the device is of cylindrical form, version II is of same construction as version I. Hence, all construction elements shown in Fig. 3 were used also in version II and are labeled with the same symbols as given in Fig. 3. Contrary to the cylindrical probe coil in version I, the rf coil of version II is saddle-shaped[8] to adjust the direction of the rf field perpendicular to the static field of the superconducting magnet which lies parallel to the direction of deformation. Summarizing, the data of version II of the tensile testing NMR apparatus are the same as that of version I enumerated in the last section.

II. PERFORMANCE OF THE APPARATUS

In the following the efficiency of the total system is demonstrated by an *in situ* experiment carried out under extreme conditions. The experiment was performed with version I of the apparatus at $T > 80$ K on a single rectangular ultrapure (5N) aluminum foil of size 27 mm $\times$ 12 mm $\times$ 50 μm in order to study the microscopic details of dislocations in the specimen. The deformation rate of the sample during the actual experiment was very large, namely 1.6 s^{-1}. Further information of the physical

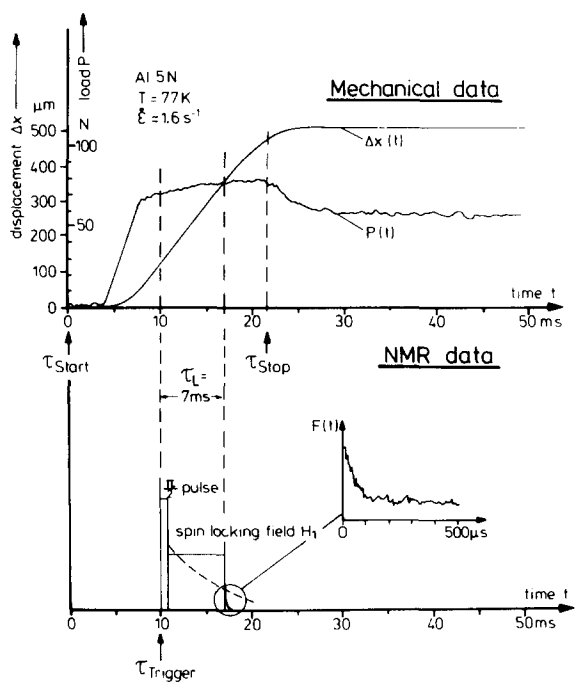

FIG. 5. Displacement Δx, load P, rf-pulse sequence ($\pi/2$ pulse followed by a locking field of strength H_1), and ^{27}Al free induction decay signal $F(t)$ as a function of time during an *in situ* NMR tensile experiment on an aluminum foil (see text).

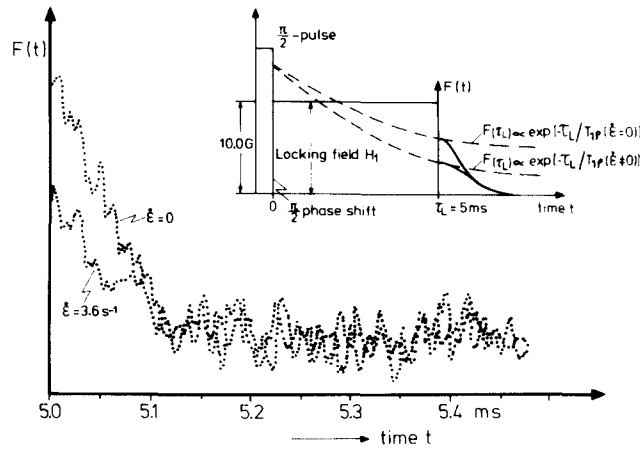

FIG. 6. Result of an *in situ* NMR tensile experiment showing the ^{27}Al free induction decays $F(t)$ in aluminum after a spin-locking sequence with zero and finite plastic strain rate $\dot{\epsilon}$. From the measurement $T_{1\rho}(\dot{\epsilon} = 0) = 25.0$ ms and $T_{1\rho}(\dot{\epsilon} = 3.6\ s^{-1}) = 7.2$ ms is obtained.

background of such experiments may be obtained from Ref. 4. Figure 5 shows the acting load P, the resulting displacement Δx, the rf pulse sequence consisting of a $\pi/2$ pulse followed by a locking field H_1, and the ^{27}Al free induction signal $F(t)$ in the experiment as a function of time. The rf pulse sequence which measures the spin-lattice relaxation time in the rotating frame, $T_{1\rho}$, of the ^{27}Al nuclei (see also Fig. 6) is applied after the delay time τ_{Trigger}. The delay is determined by the duration of the pure elastic deformation which can be obtained by the $P(t)$ curve. The trigger signal is generated by the digital function generator (see Fig. 1). As depicted in Fig. 5, the $T_{1\rho}$ measurement is carried out in a short time interval of 7 ms, where the displacement Δx is proportional to time t, resulting in a constant deformation rate of the sample of 1.6 s^{-1}. Furthermore, the acting load P is nearly constant at that time interval, particularly for stage II of the stress-strain curve of aluminum. Figure 6 shows further details of the single shot $T_{1\rho}$ measurement during the actual deformation carried out by means of the spin-locking technique. A $\pi/2$ pulse with an rf field large compared to the local fields in the sample along the x direction rotates the nuclear magnetization from the direction of the static magnetic field to the y direction. Immediately after the pulse, the rf field is phase shifted by $\pi/2$ and reduced to a value of H_1. Now $\vec{H}_1$ lies parallel to the direction of the nuclear magnetization; the magnetization is called "locked" in a frame rotating with the Larmor frequency ω_0. With respect to the rotating frame, H_1 plays the role of a time-independent field. Consequently, the rotating magnetization relaxes parallel to the locking field H_1 with a time constant $T_{1\rho}$, the relaxation time in the rotating frame. To measure $T_{1\rho}$, the nuclear magnetization is allowed to decrease in the presence of the locking field H_1 for some time t, then H_1 is turned off and the initial height (or the total area) of the nuclear free induction decay signal $F(t)$ is measured. According to Fig. 6 one has for $t = \tau_L$

$$F(\tau_L) = F(0)\exp(-\tau_L/T_{1\rho}). \quad (2)$$

The figure shows the free induction decays $F(t)$ after the spin-locking sequence with $\dot{\epsilon} = 0$ and with $\dot{\epsilon} = 3.6\ s^{-1}$, a finite plastic strain rate. Obviously an applied strain rate $\dot{\epsilon}$ causes a significant reduction in the relaxation time $T_{1\rho}$ due to the motion of dislocations. An evaluation of the experiment leads to $T_{1\rho}(\dot{\epsilon} = 0) = 25.0$ ms and $T_{1\rho}(\dot{\epsilon} = 3.6\ s^{-1}) = 7.2$ ms, respectively. According to Eq. (1), from both the data, a dislocation induced contribution to the relaxation rate of 100 s^{-1} is obtained.

It should be noted that a larger number of different investigations on dislocation dynamics has been carried out in the past by means of the NMR tensile testing apparatus described here. Only a few of them are described in Refs. 1–4.

ACKNOWLEDGMENTS

The work is part of the research program of the Foundation for Fundamental Research on Matter (F.O.M.–Utrecht) and has been made possible by financial support from the Netherlands Organization for the Advancement of Pure Research (Z.W.O.–The Hague) and the Deutsche Forschungsgemeinschaft, West Germany.

[1] W. H. M. Alsem, J. Th. M. De Hosson, R. Muenter, H. Tamler, and O. Kanert, Philos. Mag. **46,** 469 (1982).
[2] W. H. M. Alsem, J. Th. M. De Hosson, H. Tamler, and O. Kanert, Philos. Mag. **46,** 451 (1982).
[3] H. Tamler, H. J. Hackelöer, O. Kanert, W. H. M. Alsem, and J. Th. M. De Hosson, in *Nuclear and Electron Resonance Spectroscopies Applied to Materials Science*, edited by E. N. Kaufmann and G. K. Shenoy (North-Holland, 1981), p. 421.
[4] H. Tamler, O. Kanert, W. H. M. Alsem, and J. Th. M. De Hosson, Acta Metall. **30,** 1528 (1982).
[5] T. C. Farrar and E. D. Becker, *Pulse and Fourier Transform NMR*, (Academic, New York, 1971).
[6] D. Wolf and O. Kanert, Phys. Rev. B **16,** 4776 (1977).
[7] E. Fukushima and S. Roeder, *Experimental Pulse NMR: A Nuts and Bolts Approach* (Addison-Wesley, London, 1981).
[8] D. I. Hoult and R. E. Richards, J. Magn. Reson. **24,** 71 (1976).